Polymer 51 (2010) 2903–2917

Contents lists available at ScienceDirect

Polymer

journal homepage: www.elsevier.com/locate/polymer

Binary blends of linear ethylene copolymers over a wide crystallinity range: Rheology, crystallization, melting and structure properties

C. Frederix [a], J.M. Lefebvre [a,**], C. Rochas [b], R. Séguéla [a,*], G. Stoclet [a]

[a] Université Lille Nord de France, Unité Matériaux Et Transformations, USTL – CNRS UMR 8207, Batiment C6, 59655 Villeneuve d'Ascq, France
[b] Centre de Recherches sur les Macromolecules Végétales, CNRS UPR 5301, BP 53, 38041 Grenoble, France

ARTICLE INFO

Article history:
Received 15 January 2010
Received in revised form
21 April 2010
Accepted 22 April 2010
Available online 29 April 2010

Keywords:
Polyethylene
Ethylene copolymers
Blends

ABSTRACT

This study deals with the physical properties of melt-compounded blends of three linear ethylene copolymers covering a large crystallinity range, namely 77% – 46% – 16% for the high density – linear low density – ultra low density copolymers, respectively. The melt behavior assessed from the zero-shear viscosity (η_o) reveals immiscibility of the three binary systems over the whole composition range. However, the change from positive to negative deviation of η_o with respect to the log-additivity mixing law as a function of composition suggests a structural transition from partial miscibility at the interface of the phase-separated domains to incompatibility. Crystallization and melting behaviors of the blends corroborate the occurrence of phase separation in the three systems. For most blends, the temperature shift of the crystallization (T_c) and melting (T_m) peaks as compared to the ones of the pure copolymers yet indicates partial miscibility in the crystalline and/or in the amorphous regions. It is pointed out that miscibility in the amorphous phase resulting from partial miscibility in the melt may, on its own, entail T_m depression of the crystals via surface free energy effect without necessarily implying cocrystallization and crystal thickness reduction. In several cases, the presence of intermediate endotherm and exotherm between the two main peaks of the melting and crystallization traces, respectively, discloses *hybrid* crystals assigned to a composition gradient at the interface of the phase-separated domains. A marked positive deviation of the upper T_c from the linear mixing rule is observed for the three systems. A nucleating effect from the interface of the phase-separated domains is suggested to promote early crystallization in the upper T_c phase. The SAXS data reveal electron density fluctuations at a much larger scale than that of the semi-crystalline structure demonstrating the occurrence of micro-phase separation in the melt prior to crystallization. Solubility of low T_m chain species in the amorphous layers of the high T_m phase is also evidenced. AFM and DMTA support micro-phase separation in the three systems and provide complementary information on the crystalline habits in the phase-separated domains of the blends.

1. Introduction

Polyethylene-based materials (PE) display a very large variety of molecular architectures in relation to various types of polymerization methods and copolymerization with diverse α-olefins [1]. Molecular architecture includes various amounts of short and long chain branches that strongly influence the crystallinity index and the organization hierarchy of the semi-crystalline structure [2,3]. As a direct consequence, a very large panel of mechanical properties from stiff plastics to thermoplastic elastomers is available. Disregarding processing-induced effects, stiffness and yield resistance are mainly governed by the crystallinity index spanning from about 75% to a few percent only [4,5]. Besides, at equivalent stiffness, the molecular architecture of PE materials strongly influences end-use properties such as tear and puncture resistance of films, creep and fatigue of bulk pieces, and stress-crack resistance as well [6–14].

Blending of PE materials as been for long a matter of investigations with the aim of optimizing the balance between melt rheology, that governs processability, and solid state behavior, that determines the use-properties. Blends of long-chain-branched low density PE (LDPE) with linear high density PE (HDPE) or linear low density PE (LLDPE) have received much more attention than any other systems regarding the fundamentals aspects of mixing, including thermodynamics of melt blending, melt rheology in

* Corresponding author. Tel.: +33 3 20 43 49 13; fax: +33 3 20 43 65 91.
** Corresponding author.
E-mail addresses: jean-marc.lefebvre@univ-lille1.fr (J.M. Lefebvre), roland.seguela@univ-lille1.fr (R. Séguéla).

0032-3861/$ – see front matter © 2010 Elsevier Ltd. All rights reserved.
doi:10.1016/j.polymer.2010.04.045

relation to phase behavior, crystallization kinetics, structural habits, melting behavior and some physical properties. Evaluation of miscibility in the melt has been often carried out from rheological data, on phenomenological bases [15,16]. Indirect structural insights on melt miscibility have also been obtained from post-solidification studies leading to controversial conclusions due to crystallization-induced morphological changes [17]. The contradictory issues mainly concern the incidence of counit nature and content on miscibility in the melt. Rheological data that actually concern the molten state have unfortunately never been confronted with direct structural data. Such direct structural studies of blends in the melt state, essentially by means of small-angle neutron scattering, are rather sparse [18–22]. The general trend is that miscibility is strongly dependent on chain architecture, namely LDPE/HDPE blends seem to be more easily miscible than LDPE/LLDPE blends in spite of the close crystallization potential of the two components of the later system. The reasons have not been clearly elucidated so far, though various explanations have been put forward in relation to the polymer characteristics. Besides, literature is rather scarce regarding optimization of the compounding parameters and stability of the resulting blends [23–25].

Things are somewhat clearer regarding miscibility in the solid state of LDPE/HDPE and LDPE/LLDPE blends due to direct experimental access to structure determination. The components of immiscible blends in the melt crystallize individually whereas miscible blends are likely to display either cocrystallization or phase separation during the crystallization stage. Cocrystallization of miscible blends has been often reported to occur upon fast cooling from the melt. Upon slow cooling, it turned out that chain species having very different crystallization potential undergo phase separation at the scale of the crystalline lamellae [26–32], the respective lamellae of the unlike chains being seemingly distributed at random [26].

Academic studies dealing with the mixing of linear PE materials are not much profuse. The general trend is that even in case of melt miscibility, binary blends of architecturally different chains having intrinsically different crystallization capabilities (kinetics, crystal size, crystallinity, etc…) may undergo crystallization-induced phase separation during the cooling step when the unlike chain species cannot find a structural consensus. Indeed, regarding copolymers with short chain branches (SCB) longer than ethyl group, it has been extensively shown that the counits are excluded from the crystal so that only the methylene chain segments between SCB can contribute to the buildup of crystalline lamellae (*e.g.,* Ref. [33] and references therein). Then, the consensus consists in finding an optimum crystal thickness in which the methylene segments of the unlike chains can cocrystallize by chain-folding [24,27,34–36]. This phenomenon is noticeably evidenced from the crystallization and melting behavior of highly heterogeneous Ziegler–Natta copolymers that are analogous to blends of several copolymers having various counit contents. Indeed, such copolymers display a conspicuous depression of both the peak crystallization temperature and melting point as compared with the more crystalline fractions obtained by TREF [37–42] that demonstrates the occurrence of cocrystallization. However, this is a necessary but not sufficient condition. Indeed, as in the case of LDPE-based blends, it has been shown that homogeneous blends of linear copolymers capable of cocrystallization under fast cooling from the melt may undergo crystallization-induced phase separation under slow cooling conditions due to the propensity of every chain species to crystallize according to its own structural habits if enough time is given for chain diffusion (this point will be further discussed at various occasions in the text).

The present paper deals with the study of rheological, thermal, structural and dynamic mechanical behaviors of mixtures of linear PE materials having different chain architectures and crystallization potentials. It contributes understanding the compatibility in the melt- and the solid state of chemically close but physically different PE materials spanning an extremely large crystallinity range, *i.e.,* from 16% to 77%. Combining different investigation methods allows cross-checking the conclusions.

2. Experimental

2.1. Materials

The polymers under investigation consist of a Ziegler–Natta high density ethylene–hexene copolymer (HD) from Total Petrochemicals, a linear low density ethylene–octene copolymer (LL) and an ultra low density ethylene–octene copolymer (UL) from DOW Chemicals, both issued from the metallocene catalysis. The HD copolymer is a cascade-reactor bimodal compound consisting of an actual homopolymer and a random copolymer with higher counit content than the average. The molecular and physical characteristics of the three materials provided by the manufacturers are given in Table 1. Better insight of the molecular structure of the HD bimodal copolymer can be borrowed from some previous papers regarding the same material or similar ones [43,44]. The presence of an ethylene–hexene copolymer having a counit content, ξ, greater than the average value in the HD copolymer is expected to be a favorable factor for compatibilisation with the counit-rich low density copolymers. Such bimodal copolymers are well known to retain through melt-processing the intimate mixing of the unlike chains generated during the synthesis, owing to the high chain length [43,45].

2.2. Blend preparation

Blend compounding was carried out by melt-mixing which is a natural route for processing polymers although the often used solution-mixing may *a priori* seem more efficient to promote miscibility considering the rather high viscosity and low chain diffusion in the melt. The diagnosis from some comparative structural studies [36,46–48] is that differences are rather faint provided that some precautions are taken to favour thermodynamic equilibrium.

Binary blends of the three polymers having weight fractions 25/75, 50/50 and 75/25 were compounded using a co-rotating twin-screw microextruder from DSM-Explore (Geleen, The Netherlands) under N_2 atmosphere. The extrusion parameters were: barrel temperature = 220 °C, screw speed = 100 rpm, residence time = 10 min. The residence time was such that the screw torque reached a constant value, indicating *a priori* rheological equilibrium. A residence time of 30 min did not change the melt-mixing efficiency, as assessed from both crystallization and melting of the

Table 1
Molecular and physical characteristics of the materials: number-average molar weight, M_n; weight-average molar weight, M_w; counit content, ξ; density, ρ; zero-shear viscosity, η_o; crystal weight fraction, X_c.

Material	M_n (kDa)	M_w (kDa)	ξ (mole%)[a]	ρ (g/cm^3)[b]	η_o (Pa s)[d]	X_c (%)[c]
HD	14	174	0.1 (0.5)	0.959	115	77
LL	50	104	5.0 (25)	0.902	78	32
UL	75	150	12 (60)	0.870	22	16

[a] Hexene for HD; octene for LL and UL; between brackets is the SCB/1000 C atoms in the backbone.
[b] For compression-moulded sheets.
[c] From DSC measurements.
[d] From dynamic viscosity master curves at 180 °C, and using the Carreau–Yasuda modelling.

blends. First signs of degradation were yet clearly seen from the light brown colour of the extrudate resulting in slightly reduced overall crystallinity. The pure polymers were processed using the same extrusion conditions for comparison with the blends at equivalent thermomechanical history. Polymers and blends were further compression-moulded into 0.5 and 1 mm thick sheets at 180 °C for 10 min, before cooling at about 40 °C/min.

2.3. Dynamic melt rheology

Melt rheology was investigated on an ARES equipment from TA Instruments in the plane–plane configuration, using 2 mm thick sample discs of diameter 25 mm. Isochronal experiments were carried out every 20 °C over the temperature range 140–220 °C, in the frequency range $10^{-2} < \omega < 10^{+2}$ Hz, applying a shear strain of 1%. The dynamic viscosity, $\eta(\omega)$, and the master curves were computed according to standard methods. The reference temperature of 180 °C is that of the compression-moulding step in order to enable melt- and solid-state correlations regarding blend morphology. Zero-shear viscosity, η_0, was computed from the viscosity master curve using the phenomenological Carreau–Yasuda model [49].

$$\eta(\omega) = \eta_0\left[1 + (\lambda\omega)^{a}\right]^{(n-1)/a} \quad (1)$$

where n is the slope of the non-Newtonian domain at high ω values, λ is the characteristic time at the transition between the Newtonian and non-Newtonian regimes, and a is a fitting parameter for adjusting the transition zone between the two regimes.

2.4. DSC measurements

Differential Scanning Calorimetry (DSC) experiments were performed on a Q100-apparatus from TA Instruments, under nitrogen gas flow. The temperature and heat flow scales were calibrated using high purity indium and zinc samples according to standard procedures at the same heating rate as for the materials analyses. About 8 mg samples inserted into aluminium pans were submitted to heating and cooling cycles between −50 °C and 180 °C at a scanning rate of 10 °C/min, holding the samples for 3 min at each temperature limit. The 1st heating scan was aimed at erasing the thermomechanical history due to compounding and sheet moulding, as well as physical aging due to storage at RT. The subsequent cooling and 2nd heating scans were recorded for analysing the crystallization and melting of the polymers and blends. Heating scans were also recorded after cooling at various rates in the range 1–50 °C/min for probing the eventuality of crystallization-induced segregation of the blends in case structural equilibrium was not fulfilled in the moulded samples. All measurements were performed several times, as indicated at the top of Figs. 4b, 8b and 10b, using a new specimen for every run. The crystal weight fraction was computed from the melting enthalpy of the samples, using $\Delta H_f^\circ = 290$ J/g for the melting of the perfect polyethylene orthorhombic crystal [50]. The ΔH_f° drop with decreasing melting point [50] was neglected, as often assumed in literature. The ΔH_f° drop due to counit inclusion [51,52] was also ignored considering that SCB longer than ethyl are largely excluded from the crystal (see [33] and refs therein).

Dependence of the melting point on blend structure was qualitatively discussed via the Gibbs–Thomson relation [53]

$$T_m = T_m^\circ\left[1 - 2\sigma_e/\left(\Delta H_f^\circ \rho_c L_c\right)\right] \quad (2)$$

where T_m and T_m° are the experimental and the thermodynamic melting points, respectively, σ_e is the surface free energy of the chain-folding surfaces of the crystalline lamellae, ρ_c is the crystal density and L_c is the crystal lamella thickness.

For the sake of a better insight into the structural features of the blends, every heating and cooling traces have been compared with the curves computed from the linear combination of the experimental traces from the components. Only the linear slope of the DSC recordings has been readjusted in order to match the onset ($T < -40$ °C) and the end ($T > +120$ °C) of the computed and experimental traces.

2.5. DMTA measurements

A RSA3 apparatus from TA Instruments was used for Dynamic Mechanical Thermo-Analysis (DMTA) in tensile mode. The rectangular test pieces were 10 mm in gauge length, 4 mm wide a 0.5 mm thick. Measurements were carried out at 1 Hz frequency, in the temperature range −140/+120 °C. The dynamic strain amplitude of about 0.1% was determined after preliminary assessment of the linear viscoelastic strain domain of the pure copolymers. The static stress was 10% greater than the dynamic stress amplitude in order to avoid buckling. All experiments have been carried out in duplicate with two different samples. Similar measurements have also been performed in torsion mode on an ARES apparatus from TA Instruments for the sake of cross-checking some unusual findings.

2.6. AFM structural analysis

Atomic Force Microscopy (AFM) observations were performed at RT on a Dimension 3100 apparatus (Digital Instruments) operated in *Tapping Mode*. Special care was taken to control the tip penetration depth with regard to the size of the crystalline and amorphous layers in order to optimize the *phase* contrast. The 100 μm thick samples were slow cooled from the melt under nitrogen, with free upper surface in order to generate a crystallization-induced morphological fingerprint. More experimental details are given elsewhere [54].

2.7. SAXS measurements

Small-Angle X-ray Scattering (WAXS) experiments have been carried out on the BM2 beamline of the European Synchrotron Radiation Facility (Grenoble, France) equipped with a 0.1 mm point-focusing collimation and a CCD camera from Princeton Instruments, using an X-ray wavelength $\lambda = 1.54$ Å. The 2D-patterns were corrected for background scattering, geometry and intensity distortions of the detector, and normalized with regard to sample thickness by using the transmission coefficient. The intensity profiles, $I(q)$, versus scattering vector, q, were computed by azimuthal integration of the 2D-patterns using the FIT2D software. Reproducibility of the SAXS experiments has been checked on different specimens of the pure copolymer samples that generated $I(q)$ profiles with less than 3% deviation in the correlation peak position and a maximum deviation of 5% in intensity. The most probable long period, L_p, was computed from the Lorentz-corrected intensity profiles $Iq^2(q)$ using the Bragg relation $L_p = 2\pi/q_{max}$, where q_{max} is the scattering vector at the peak maximum.

3. Melt rheology

It is worth mentioning first that the different nature of the counits in the various copolymers, namely octene for LL and UL versus hexene for HD, should not *a priori* influence the phase behavior of the blends. Indeed, according to Reichart et al. [21], the interaction strength that rules the mixing thermodynamics of ethylene copolymers depends much more on the concentration of

the counits than on their nature. Some influence of the SCB length on binary blend miscibility in the melt has yet been reported without physical explanation [55,56].

Fig. 1 reports the η_o data for the three systems as a function of blend composition. It is to be noticed first that the η_o data for the pure copolymers are ranking in the same order as the decreasing counit content (Table 1). This is purely fortuitous. Second, none of the three systems obeys a log-additivity mixing rule relevant to miscibility. The η_o versus composition curves have a sigmoidal shape that is an indication of structural changes in the molten blends as a function of composition. It is worth noticing that, though the choice of the reference temperature for the master curves has an incidence on the η_o values, it does not change the observed evolutions as a function of composition for the three systems. Therefore, the following discussion would hold for any temperature in the range 140–220 °C.

The UL/LL system displays a quite large amplitude of η_o variation. In the UL-rich composition range, the fairly good log-additivity mixing rule suggests miscibility of the UL and LL chains, as often claimed in literature in similar circumstances, for various kinds of blends including PE-based polymers [15,16]. In contrast, the η_o positive deviation from the linear mixing law that is observed in the LL-rich range is a common phenomenon often ascribed to an emulsion-like behavior, otherwise immiscibility [36,56–58]. Besides, the positive sign and the high amplitude of this deviation are indicative of strongly favorable interactions at the interfaces of the segregated phases. In previous studies regarding PE-based blends, no particular endeavor was made for explaining the positive viscosity deviation on molecular grounds. Considering that only van der Waals interactions can develop between the UL and LL chains of the present system, a miscibility transition zone between the UL-rich and LL-rich phases is likely to account for favorable interactions via diffusion of chains through the interface and intertwining. Such a UL/LL miscibility gradient may operate via the chain species having similar molecular architecture in the two copolymers, namely similar counit contents. This assumption borrows from the observation of non-uniform composition distribution in both the UL and LL metallocene copolymers having different average values of counit contents, as will be shown in the next section. In support to the present interpretation of the η_o positive deviation, it is worth noticing several rheological studies of various immiscible polymer blends that reported a significant increase of dynamic viscosity owing to interfacial compatibilization, noticeable via block or grafted amphiphilic copolymers that buildup actual molecular interconnections and chain entanglements through the interface [59–63].

The UL/HD system exhibits the same type of dual behavior suggesting phase separation (Fig. 1). However, the η_o positive deviation from the log-additive mixing rule in the HD-rich range is much less pronounced than in the previous system in spite of the somewhat higher viscosity difference between the two copolymers, *i.e.*, $\Delta\log\eta_o = 0.7$ for UL/HD versus $\Delta\log\eta_o = 0.5$ for UL/LL. This finding could *a priori* be taken as an indication of better

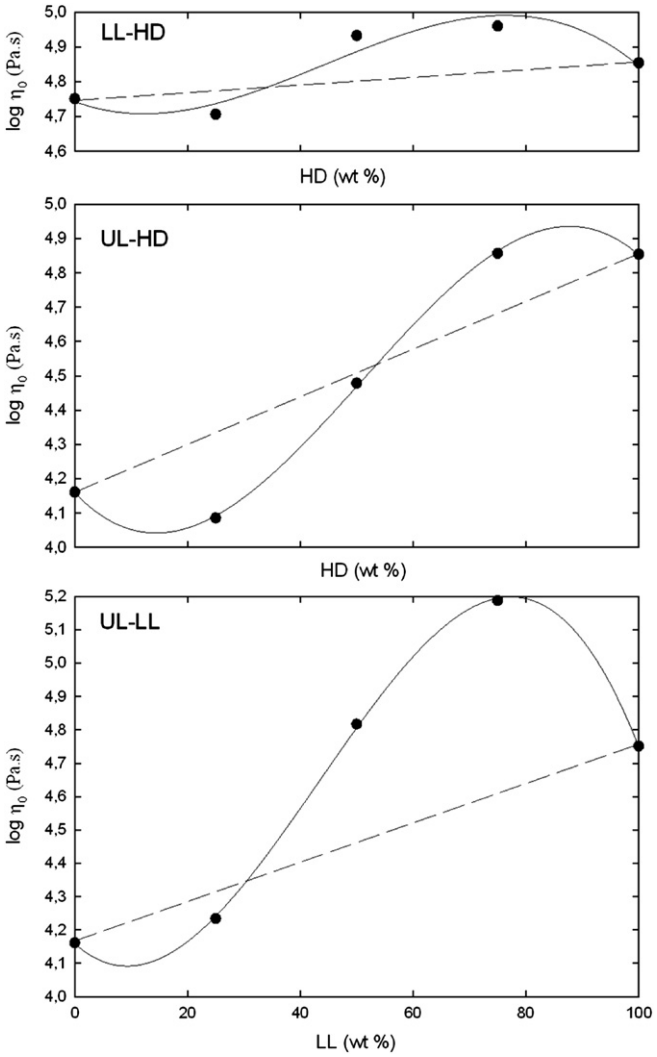

Fig. 1. Zero-shear viscosity, η_o, at 160 °C for the UL/LL, UL/HD and LL/HD blends as a function of composition.

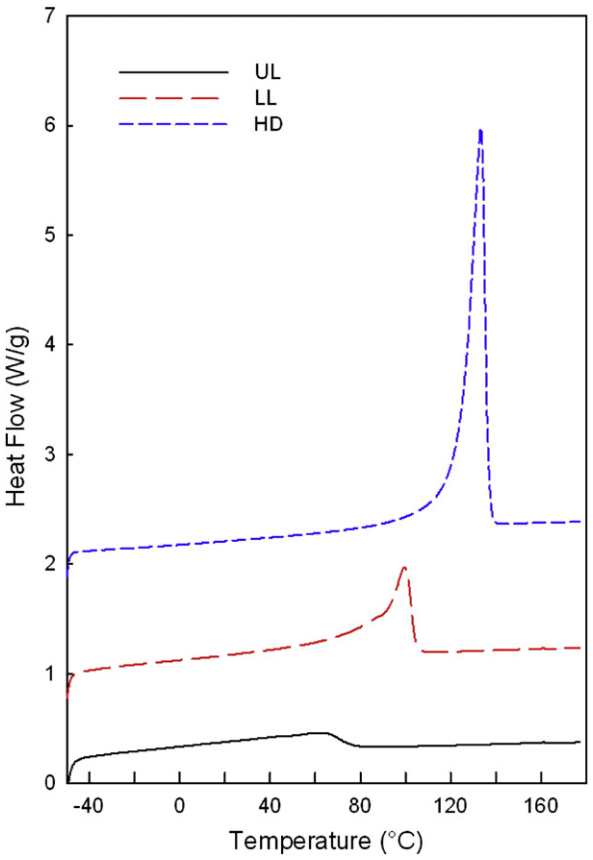

Fig. 2. DSC heating traces of the three pure polymers recorded after continuous cooling at 10 °C/min from 180 °C down to −50 °C.

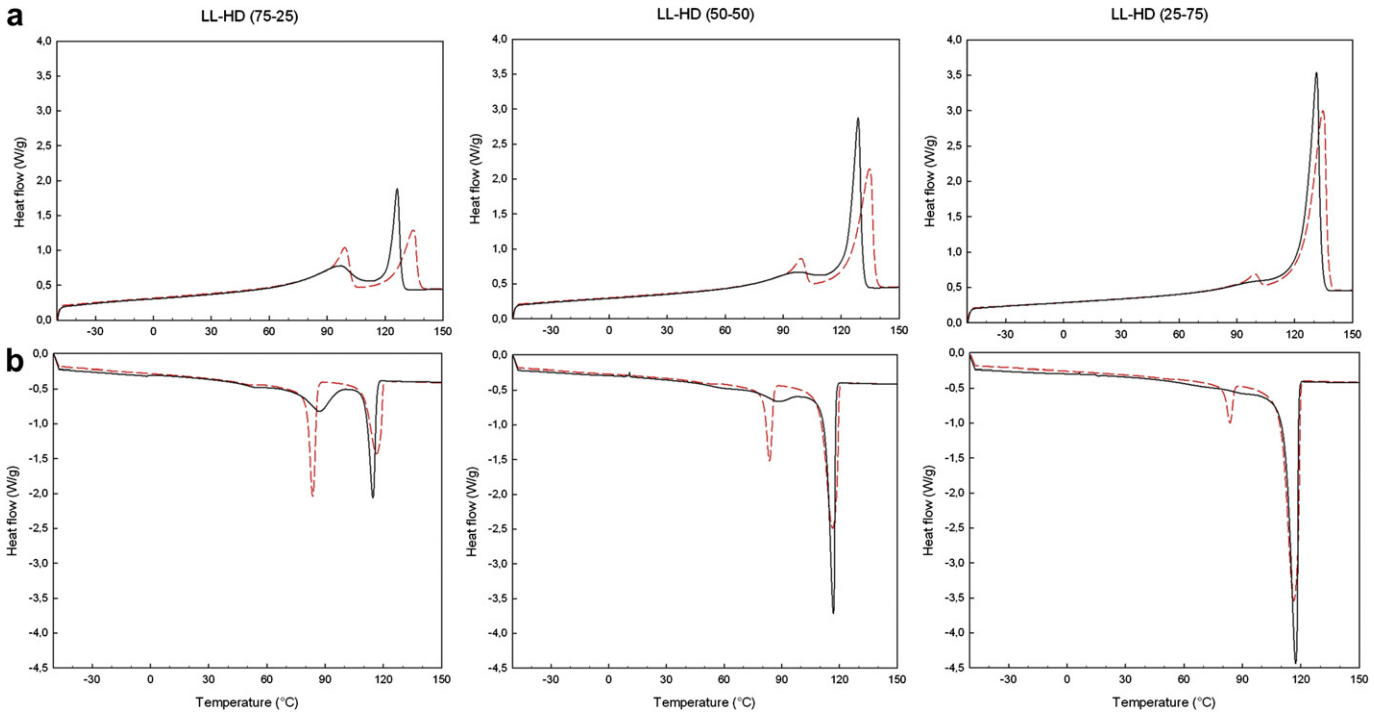

Fig. 3. DSC (a) heating traces and (b) cooling traces of the LL/HD blends (the dotted lines stand for the computed linear combination of the experimental traces of the individual copolymers taking account of the copolymer weight fractions).

compatibility of the UL/HD system as compared to the LL/HD one. Alternatively, one may suspect similar immiscibility trend for the two systems but weaker interfacial interactions for the former one. The 1st issue is contradictory with a number of studies concluding that an increase in SCB content reduces melt compatibility of linear copolymers with LDPE. This is particularly true for copolymers with SCB >40/1000 C backbone atoms [20,25], that is precisely the case of the UL copolymer. Relying on indirect solid-state investigations, Hill and Barham [46,55,64–66] have extensively reported that the miscibility of copolymer blends with HDPE in the melt surprisingly increases with increasing counit content in the copolymer. Hussein et al. [32] also observed increased miscibility of LDPE–LLDPE blends with increasing SCB in the LLDPE component. Kwak et al. [67] and Guimaraes et al. [68] concluded for melt miscibility of HDPE/ULDPE blends close to the present binary UL/HD system. This is rather coherent with the 1st proposal, although not strictly consistent. All these puzzling data do not allow us to argue further in favour of either of the two above structural hypotheses.

A striking behavior of the UL/HD system is the pronounced negative deviation of η_o to the log-additivity rule in the UL-rich range. This behavior has been scarcely reported in the case of PE-based blends [15,16,36,58]. It has been ascribed to interfacial sliding during the experiments due to lacking interfacial interactions. Recent works regarding layered blends of immiscible polymers with no specific interactions, including a polyolefin, have indeed shown that dynamic viscosity of the multilayers actually drops with regard to that of the components due to the sliding of the layers [62,69,70]. In the present case, such a molecular scheme would mean that the segregated phases in the UL-rich composition range exclude interfacial molecular interconnections, may be due to the large ξ difference between UL and HD chains. This is again rather consistent (although not in full agreement) with Hill–Barham's conclusion that an actual phase separation loop exists in this region of the phase diagram.

Regarding the LL/HD system, the data of Fig. 1 show quite moderate deviation of the blend viscosity from the log-additivity mixing rule as compared with the two previous systems. Besides the rather small $\Delta\log\eta_o$ value for this system, the two copolymers have close chain lengths and moderate ξ difference that let foresee good compatibility.

From a general point of view, the three binary systems display a similar sigmoidal shape of the η_o versus composition curve, with negative deviation on the high ξ copolymer side and positive deviation on the low ξ copolymer side. Obviously, this cannot be due to the η_o difference between the two components since the η_o deviation from linearity is maximum for the UL/LL system which displays the smaller $\Delta\log\eta_o$ of the three binary systems. This gives indication of thermodynamic immiscibility combined with different kinds of interfacial interactions on either side of the phase diagram. The lower the ξ difference of the copolymers, the more favorable the interactions between the phase-separated domains in the blends.

4. Melting and crystallization

4.1. Pure copolymers

Fig. 2 shows the DSC heating traces of the three pure polymers. The value T_m = 133 °C for HD is typical of a high crystallinity material. Regarding the UL and LL copolymers, the broad melting endotherm is indicative of a non-uniform composition distribution (CD). Although ethylene copolymers issued from the metallocene technology display much narrower CD and MWD than their Ziegler–Natta parents, significant CD is observed at high counit content [71,72], depending on the nature and structure of the catalyst. The extent of the melting endotherm far below RT for the UL copolymers is relevant to highly counit-rich chains that crystallize upon cooling below RT or by aging/annealing at RT for long periods. This latter treatment results in the occurrence of a melting peak a few °C above RT [47,73], the amplitude of which depends on aging time. This is the reason why the DSC heating traces reported in the present study are the ones recorded after continuous cooling from 180 °C down to −50 °C.

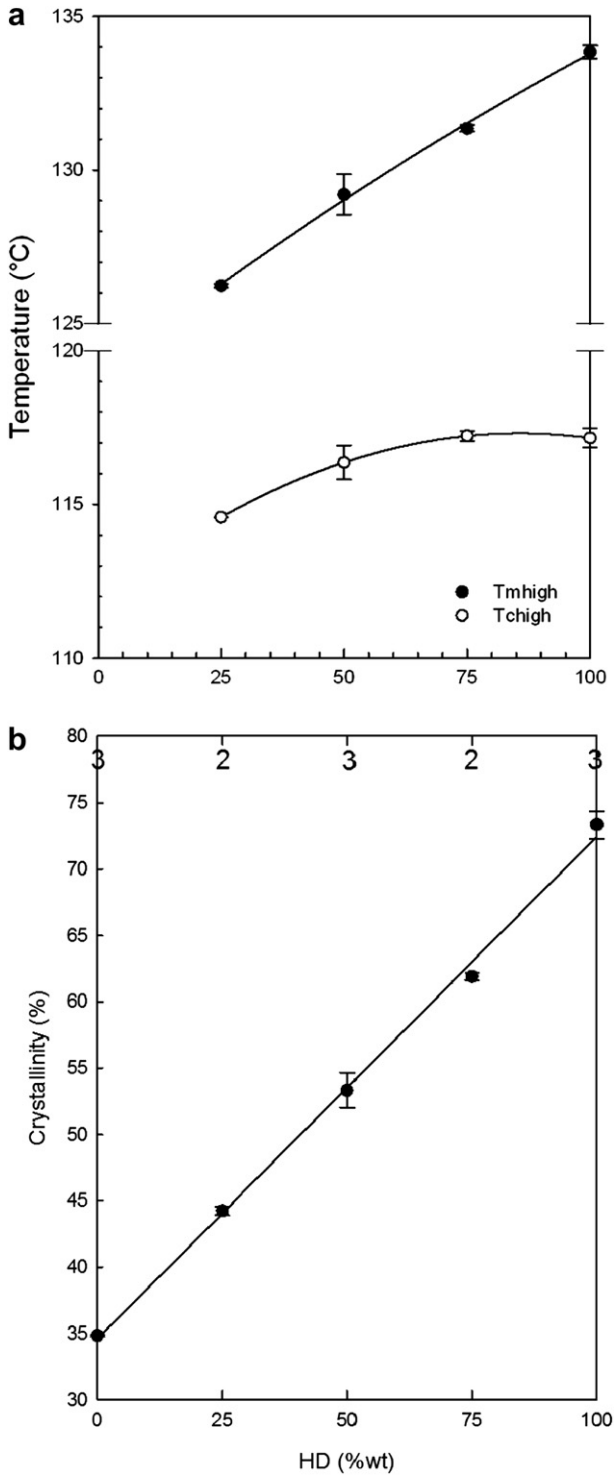

Fig. 4. Variation with composition of (a) the high temperature melting peak, T_m^{high}, and the high temperature crystallization, T_c^{high}, peak of the LL/HD blends, and (b) the overall crystallinity index (digits at the top of Fig. 4b indicate the number of measurements for each data point).

4.2. LL/HD blends

Fig. 3 shows the DSC cooling and the heating traces of the LL/HD blends. Also shown on this figure are the curves computed from a linear combination of the traces of the pure copolymers. The experimental heating curves of the blends display a high temperature (HT) and a low temperature (LT) melting endotherms that

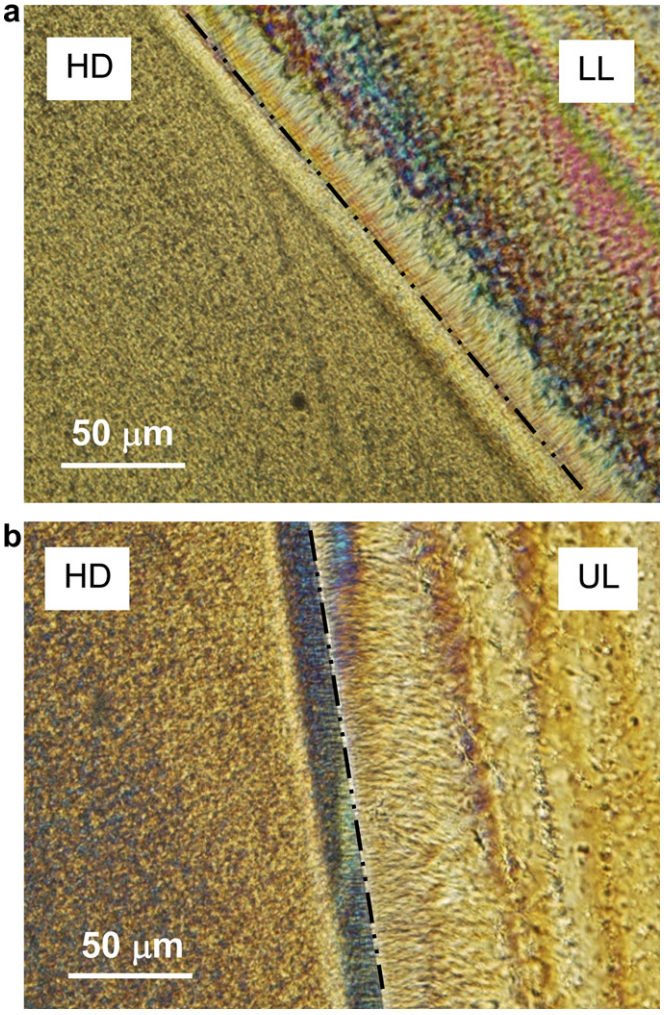

Fig. 5. Optical micrographs of cross-section slices from (a) LL/DH and (b) UL/HD bilayer sheets after welding via compression under very light pressure at 180 °C.

roughly correspond to the two individual copolymers. The experimental cooling curves display a clear cut HT crystallization exotherm and a very broad LT exotherm that also roughly correspond to the two individual copolymers. This is evidence of phase separation in the solid state. Moreover, the crystallization behavior enables assuming that micro-phase separation was already present in the melt prior to the crystallization completion, in the circumstances of the present preparation conditions of the materials. Indeed, if miscibility prevailed in the melt, segregation of the unlike chains would not have enough time to occur during the continuous cooling.

Regarding more specifically the heating traces, the HT melting peak (T_m^{high}) exhibits a nearly linear depression with respect to the pure HD copolymer as shown in Fig. 4a. This suggests partial miscibility of LL chains in the HD-rich phase of the blends. This could be assigned to a thickness reduction of the crystals in HD-rich phase with respect to the pure HD copolymer due to cocrystallization, as often claimed in literature for similar situations [27–35,57,74], though the correlation with the Gibbs–Thomson equation was very rarely referred to in justification. Cocrystallization indeed involves accommodation in the same crystallites of crystallizable methylene sequences from the lower melting point copolymer that have smaller average length than the ones from the high melting point copolymer [27,40,75]. It straightforwardly ensues a drop of the average crystal thickness and a concomitant melting point depression. Under such circumstances, miscibility

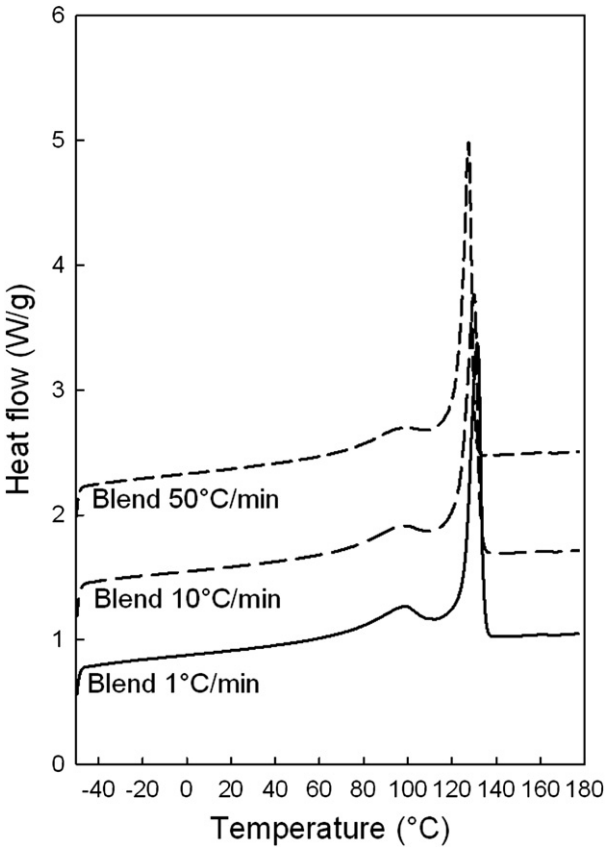

Fig. 6. DSC heating traces of the 50/50 LL/HD blend crystallized at various cooling rates.

would concern both the crystalline and the amorphous regions since the gyration radius of the chain coils embraces several crystalline lamellae in the solid state [76].

A physical phenomenon generally ignored regarding crystallizable blends is that, according to the Gibbs–Thomson equation, a change in the crystal surface free energy as a result of compositional change in the amorphous phase may also trigger a melting point depression in a blend, without necessarily implying crystal thickness decrease. Indeed, fringed-micelle crystals from counit-rich ethylene copolymers have higher σ_e than regularly chain-folded lamellar crystals from homopolyethylene: the limiting σ_e values are about 0.07 J/m^2 for chain-folded crystals and 0.24 J/m^2 for fringed-micelles (see Ref. [77] and references therein). Therefore, in the present case, increasing LL chain concentration in the amorphous regions of HD-rich phase should result in higher σ_e in this phase, thus contributing to the T_m^{high} depression and to the amplification of this phenomenon with increasing LL content. In such a case, miscibility may eventually be restricted to the amorphous phase only, after exclusion of the LL chains from the crystalline region during the crystallization step. This means that melting point depression in the LL/HD blends does not necessarily mean that cocrystallization has occurred, unlike usually assumed in literature for PE-based blends.

The fact that the LT endotherm (Fig. 3a) has systematically lower amplitude than that of the pure LL copolymer suggests that LL chains are missing in the LL-rich phase of the three blends. This phenomenon is less obvious for the HT endotherm, indicating that some HD chains are missing in the HD-rich phase. Moreover, it is noteworthy that the endothermic signal recorded in the temperature range between the HT and LT endotherms of the blends is higher on the experimental traces than on the computed ones. This is an indication of the melting of *hybrid* crystals having an intermediate composition between the two main crystallite populations in the blends. This is a hint that a composition gradient exists between the HD-rich and LL-rich phases of the blends, over the whole composition range of the LL/HD phase diagram, this gradient zone being composed of the HD chains missing from the HD-rich phase and the LL chains missing from the LL-rich phase. These HD and LL chains capable of cocrystallization have quite likely close ξ values.

Regarding the cooling traces (Fig. 3b), the HT crystallization peak exhibits a depression trend (Fig. 4a) that roughly confirms the partial miscibility of LL chains in the HD-rich phase in the melt, and

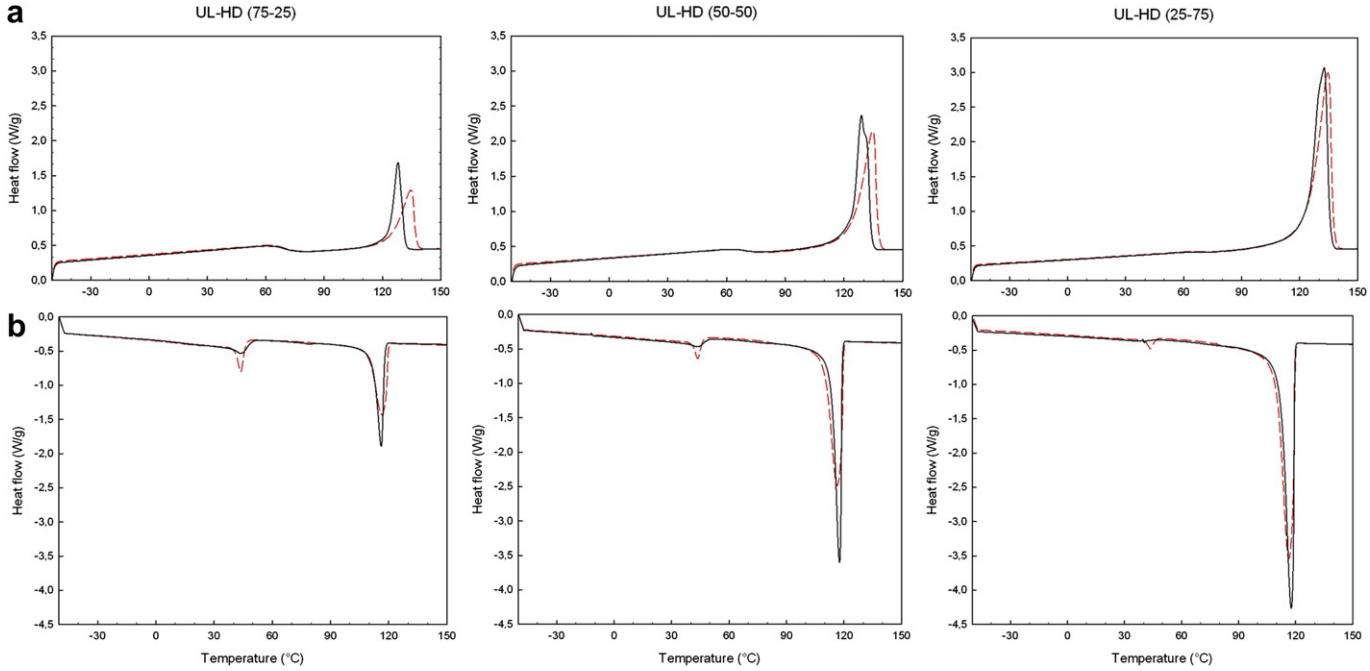

Fig. 7. DSC (a) heating traces and (b) cooling traces of the UL/HD blends (the dotted lines stand for the computed linear combination of the experimental traces of the individual copolymers taking account of the copolymer weight fractions).

the cocrystallization in the solid state. However, the 25/75 blend roughly displays the same T_c^{high} as the pure HD (Fig. 4a) which strongly contrasts with the T_m^{high} depression. There is therefore a need to consider that some specific factor promotes crystal nucleation and growth in the HD-rich phase, but does not intervene in the melting process. The narrowing of the HT crystallization exotherm of this blend (Fig. 3b) is an additional hint of an increase in the global crystallization rate. In the case of rubber-toughened semi-crystalline polymers, the matrix–particle interfaces have been shown to play an active nucleation role even in the absence of strong interactions [78–80]. This phenomenon also occurs when molten polymers are dispersed in non-solvents, as reported for polyethylene [81,82]. Finally, bilayer films have been recognized to exhibit interface-induced nucleation in the semi-crystalline layer in contact with an amorphous [83] or molten polymer [84].

Much akin to Muratoglu et al.'s work [83], an experimental evidence has been provided for interface-induced nucleation in the case of a bilayer sheet of the HD and LL copolymers prepared via melt welding. Fig. 5a shows an optical micrograph of a cross-section slice of the HD/LL bilayer sheet. A conspicuous trans-crystallization of the LL layer starting from the LL/HD interface gives clear evidence of the nucleating effect of the HD crystals, as already reported for similar LLDPE/HDPE blends [85] and LDPE/HDPE blends as well [86]. This is probably due to an epitaxy phenomenon as evidenced by Loos et al. [85] from transmission electron microscopy. A less obvious but notwithstanding clear trans-crystallization of the HD layer also appears on this micrograph, suggesting an interfacial nucleation effect. It is worth mentioning that the LL layer was still in the melt stateat the time the crystallization of the HD layer occurred. The physical origin of this interface-promoted nucleation might be either interfacial free energy [78] or interfacial topological constraints [82], according to previous works. Although not clear elucidated, this phenomenon gives support to the hypothesis of an interface-induced nucleation in the HD-rich phase in the 25/75 blend. Considering moreover the ten micron thickness of the trans-crystallization zone in the HD layer of the bilayer, one may reasonably expect that the trans-crystallization phenomenon is liable to invade the whole volume of the HD-rich phase-separated domains.

It is worth noticing Xu et al.'s study [31,74] of partly miscible LDPE blends with either heterogeneous Ziegler–Natta or homogeneous metallocene copolymers of medium density. These authors reported an upward shift of the crystallization temperature of the heterogeneous copolymer in the blend as compared to the pure copolymer, and of the melting point as well. The phenomenon was ascribed to the transfer of the counit-rich chains of the copolymer to the LDPE-rich phase. By contrast, the blends with the homogeneous copolymers exhibited the usual depression of both crystallization and melting points due to cocrystallization. In spite of evidences of mutual miscibility of the unlike chains in the phase-separated domains of the present LL/HD system, Xu et al.'s scenario may not be transposed to the T_c^{high} positive deviation in the 25/75 blend considering the T_m^{high} monotonic decrease.

The strong broadening of the LT exotherm on its high temperature side (Fig. 3b) reveals the growth of a crystallite population with very wide thickness distribution that supports the existence of a transition zone with large composition gradient between the HD-rich and the LL-rich phases, as previously concluded from the melt behavior [31].

In Fig. 6 are reported the DSC heating traces of the 50/50 LL/HD blend crystallized under various cooling rates. Whereas the LT endotherm displays no significant changes within experimental accuracy, the HT melting peak slightly shifts upward with decreasing cooling rate. The two other blends display the same trend. The fact that the pure HD copolymer (not displayed) also exhibits the same trend means that the phenomenon results from

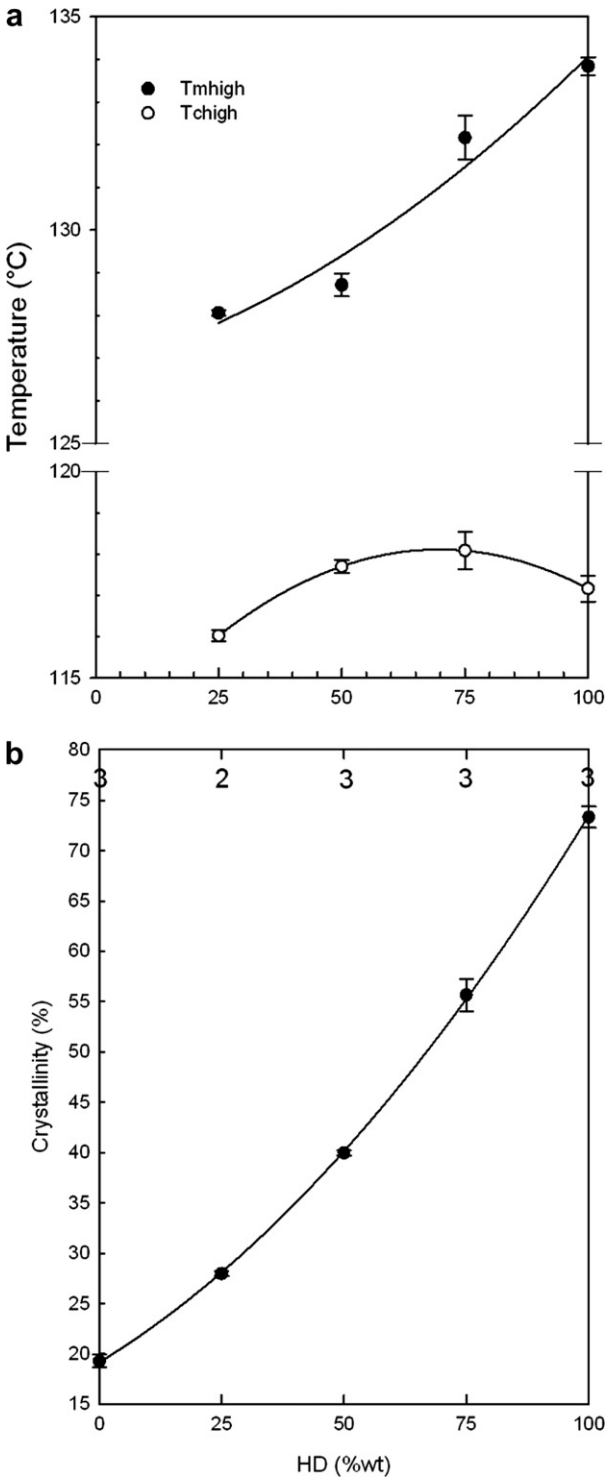

Fig. 8. Variation with composition of (a) the high temperature melting peak, T_m^{high}, and the high temperature crystallization, T_c^{high}, peak of the UL/HD blends, and (b) the overall crystallinity index (digits at the top of Fig. 8b indicate the number of measurements for each data point).

an improvement in crystal perfection in relation to the more favorable crystallization conditions. These data indirectly confirm phase segregation into HD-rich and LL-rich domains and suggest that no LL chain segregation takes place in the HD-rich phase during the DSC crystallization run. One should keep in mind that all materials have undergone a crystallization step after compression-moulding, *i.e.,* prior to the DSC study.

The linear composition dependence of the global crystallinity reported in Fig. 4b suggests that the partial miscibility of the LL and HD chains in the melt due to favorable thermodynamic factors does not modify their crystallization capability in the blends, as compared to the pure copolymers. Therefore, cocrystallization in the HD-rich phase or *hybrid* crystals seem to be a means not to reduce the blend free energy, but just to preserve it.

4.3. UL/HD blends

Fig. 7 shows the DSC heating and the cooling traces of the UL/HD blends together with the traces computed from the pure copolymer data. Again, both the heating and cooling experimental traces of the blends display HT and LT first order transitions that roughly correspond to the melting and crystallization of the two individual copolymers. These are strong hints of micro-phase separation into UL-rich and HD-rich domains in the solid blends.

Regarding the melting, the fact that the LT endotherm is much similar to that of the pure UL copolymer for the three blends indicates that miscibility if any is very weak in the crystalline region of the UL-rich phase. One may suspect that miscibility in the amorphous region of the UL-rich phase is also quite low. Yet, the systematic depression of the HT melting peak (T_m^{high}) reported in Fig. 8 is indicative of partial miscibility of UL chains in the HD-rich phase. As for the previous LL/HD binary blend system, this miscibility may take place either in both the crystalline and the amorphous regions of the HD-rich phase or in the amorphous region only: in the first case, the T_m^{high} depression would result from the drop of crystal thickness due to cocrystallization, whereas in the second case it would be a consequence of an increase of the crystal surface free energy.

The cooling traces of the three blends (Fig. 7b) reveal, at first sight, no major changes in both the area and the peak temperature of the HT crystallization exotherm as compared with the pure HD copolymer, except a slight narrowing and concomitant amplitude increase. In parallel, the LT exotherm displays an obvious flattening with no measurable area modification. An acute examination of T_c^{high} (Fig. 8a) yet exhibits a highly non-linear evolution with composition that contrasts with that of T_m^{high}, as in the case of the LL/HD system. Moreover, both the 25/75 and 50/50 UL/HD blends exhibit higher T_c^{high} than the pure HD copolymer. This early crystallization in the HD-rich phase again suggests that a specific nucleating effect is operating in the blends. The optical micrograph of Fig. 5b shows that the UL/HD interface in a bilayer sheet is an active nucleation site for both components as can be judged from the trans-crystalline structure in both layers. As for the LL/HD system, the trans-crystallization of the HD-rich domains onto the HD/UL interface is an evidence that an interfacial nucleation should take place in the HD-rich domains of the blends, although the UL-rich phase was molten during the crystallization process.

Absence of distinct intermediate melting and crystallization transitions in the heating and cooling traces of the blends is an indication of very few if any *hybrid* crystals. This is a clear hint of little miscibility between UL and HD chains in the crystalline state. Therefore, the origin of the T_m^{high} depression would be rather assigned to crystal surface free energy due to partial miscibility in the amorphous phase of the HD-rich phase than to cocrystallization.

The global crystallinity of the UL/HD blends reported in Fig. 8b obeys a roughly linear relationship in perfect consistency with the observation of limited miscibility that does not restrain the crystallization capabilities of the UL and HD chain species.

4.4. UL/LL blends

Fig. 9 shows the experimental DSC cooling and heating traces of the UL/LL blends together with the computed traces from the pure copolymers. The heating curves display HT and LT melting endotherms that roughly correspond to the pure copolymers. At first

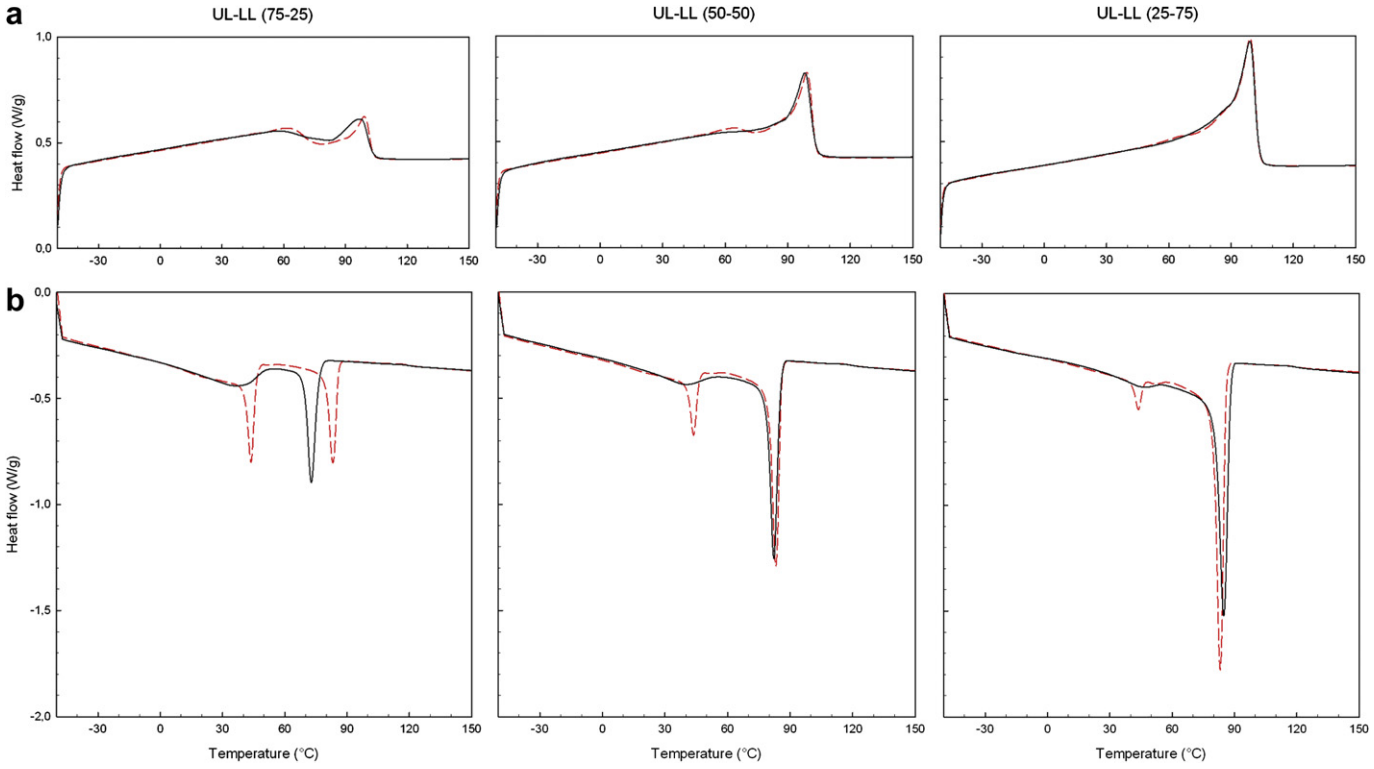

Fig. 9. DSC (a) heating traces and (b) cooling traces of the UL/LL blends (the dotted lines stand for the computed linear combination of the experimental traces of the individual copolymers taking account of the copolymer weight fractions).

sight, the rough evolution trend of the HT peak is a slight depression and broadening with respect to that of the pure LL copolymer (Fig. 9a). This suggests miscibility and possibly cocrystallization of UL chains in the LL-rich crystals, that will be further discussed below. In parallel, the LT endotherm has turned flatter, indicating that some UL chains are missing due to miscibility with LL chains. The additional endothermic contribution between the two main melting peaks reveals the melting of *hybrid* crystals that did not exist in the either of the two pure copolymers. This is evidence of a transition zone with composition gradient involving cocrystallization between the LL-rich and UL-rich phases.

The cooling traces of the blends display HT and LT crystallization exotherms that roughly correspond to the ones of the two pure copolymers (Fig. 9b). However, if the HT exotherm is very close to that of the pure LL copolymer in the 50/50 and 25/75 blends, that of the 75/25 blend is largely depressed. This is consistent with partial miscibility and cocrystallization in micro-phase-separated blends. The presence of an excess exothermic signal in the range 50–70 °C between the two main crystallization exotherms confirms that a composition gradient zone consisting of *hybrid* crystals exists between the LL-rich and UL-rich phases. The strong reduction in amplitude and area of the main peak of the LT exotherm indicates that UL chains having a lower counit content than the average value of the UL copolymer have cocrystallized with their homologous chains from the LL copolymer. This cocrystallization is the origin of the so-called *hybrid* crystals.

Fig. 10 enables close examination of the composition dependence of both T_c^{high} and T_m^{high} of the UL/LL blends. The T_c^{high} evolution exhibits a significant positive deviation from the linear mixing law, that even exceeds the crystallization point of the pure LL copolymer for the 25/75 blend. This is an indication of an early crystallization according to the previously proposed mechanism of interface-promoted nucleation. The T_m^{high} evolution (Fig. 9a) is perfectly confirmed in Fig. 10a. As for the two previous binary systems, the T_m^{high} depression for the 75/25 blend may be due to either crystal thickness reduction or to the surface energy increase as a result of miscibility of UL chain in the LL-rich phase. In contrast, T_m^{high} of the 25/75 blend slightly exceeds that of the pure LL copolymer. This may have two different sources:1) the occurrence of Xu et al.'s scenario [31,74], suggesting that some counit-rich chains of the LL copolymer have been excluded from the LL-rich phase; 2) the increase of crystal thickness as a result of early crystallization. The first hypothesis should involve a reduction of the HT melting peak area of the 25/75 blend, which is not obvious from Fig. 9a. Conversely, the second assumption will be confirmed from the DMTA experiments in the following.

Fig. 10b shows that the global crystallinity of the UL/LL blends roughly obeys a linear additivity law as for the two previous systems that confirms that, with or without cocrystallization, the crystallization potential of each species is preserved. This means that it is not possible on structural bases to raise the crystallinity of a given species via blending, thanks to cocrystallization.

A global conclusion from the DSC analysis is that the three binary systems display micro-phase separation with partial miscibility depending on the ξ difference of the two components in every system. However, DSC data only suggest that phase separation occurred in the melt prior to crystallization, they do not provide direct demonstration *per se*. Demonstration will be provided in the next section.

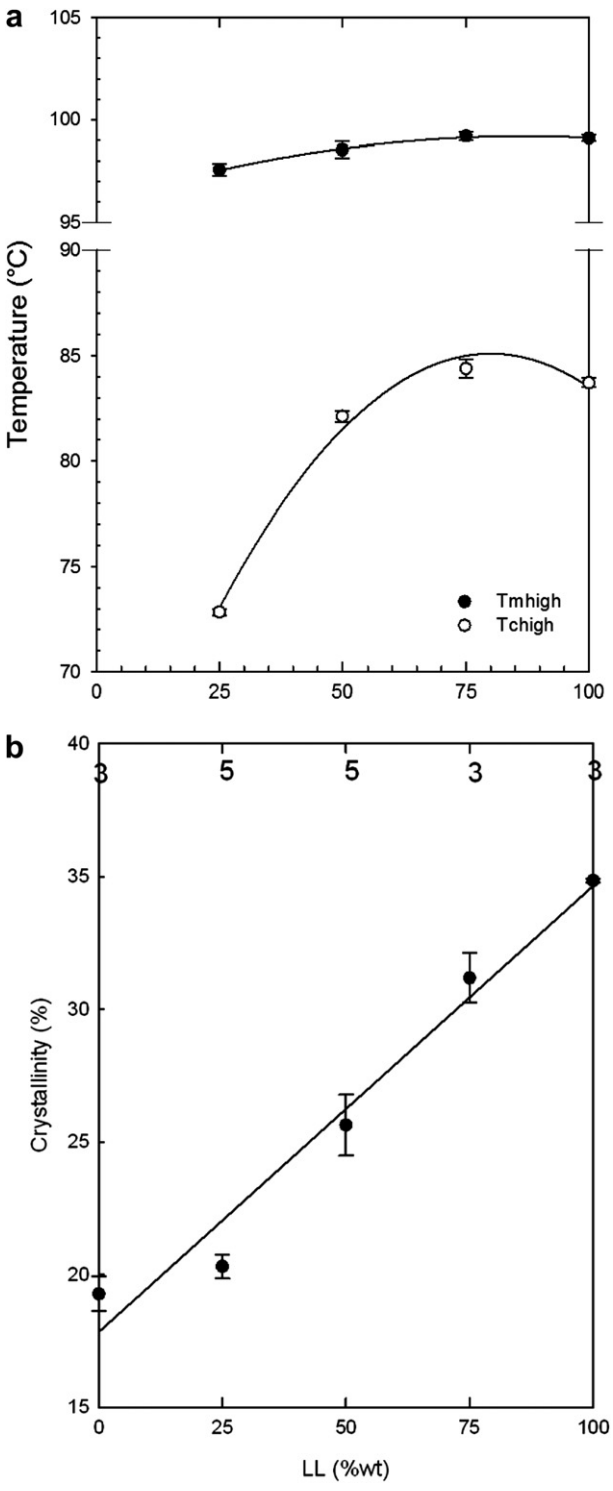

Fig. 10. Variation with composition of (a) the high temperature melting peak, T_m^{high}, and the high temperature crystallization, T_c^{high}, peak of the UL/LL blends, and (b) the overall crystallinity index (digits at the top of Fig. 10b indicate the number of measurements for each data point).

5. Morphology

5.1. SAXS analysis

Fig. 11 reports the uncorrected $I(q)$ intensity profiles and the Lorentz-corrected $Iq^2(q)$ profiles of the blends and the pure copolymers for the three binary systems. The pure copolymers exhibit a correlation peak relevant to a periodic stacking of crystallites. Moreover, in contrast to the LL and UL copolymers, the HD copolymer reveals a harmonic indicative of a highly regular stacking of lamellar crystals. The occurrence of this harmonic at about the same q value as the correlation peak of the LL and UL

copolymers may entail problems in the SAXS interpretation. The broadness of the correlation peak of the LL and UL copolymers is a hint of a very large L_p distribution related to thickness distributions of both the amorphous layers and the crystal lamellae, in agreement with the melting behavior. This finding is also consistent with previous assignments to counit-rich metallocene copolymers of a fringed-micelle structure [73,75,87] for which a regular crystal stacking is highly unlikely. The very close position of the UL and LL correlation maxima indicates very close L_p values. This does not mean yet that the two copolymers have the same most probable crystal thickness, it just means that $L_p = L_a + L_c$ is about the same with different values of both the amorphous layer thickness, L_a, and the crystal thickness, L_c. Furthermore, the strong intensity difference between the two copolymer is quite consistent with their respective crystallinity index.

A noteworthy feature of the $I(q)$ profiles is the drastic intensity upswing at very low q values for the blends as compared to the pure components. From a qualitative standpoint, this is an evidence of electronic density variations that do not exist in the pure components and having a characteristic length scale much larger than the semi-crystalline long period. In the present circumstances, this can only be due to composition heterogeneities, in support to the previous conclusion from rheology and thermal investigations that all blends exhibit micro-phase separation. It is worth noticing that similar observations has never been reported elsewhere so far. Particularly conspicuous is the intensity jump at small q for the three UL/HD blends that is consistent with the fact that this system is the one with the strongest phase separation capabilities and the greatest electronic density contrast.

Further analysis of the SAXS data is based on the Lorentz-corrected intensity profiles that is the appropriate method for quantitative studies of isotropic lamellar systems.

5.2. LL-HD system

The 25/75 blend displays a 1st correlation peak assigned to the HD copolymer. The 2nd one is a combination of the LL copolymer maximum and the HD harmonic, as revealed by its intermediate

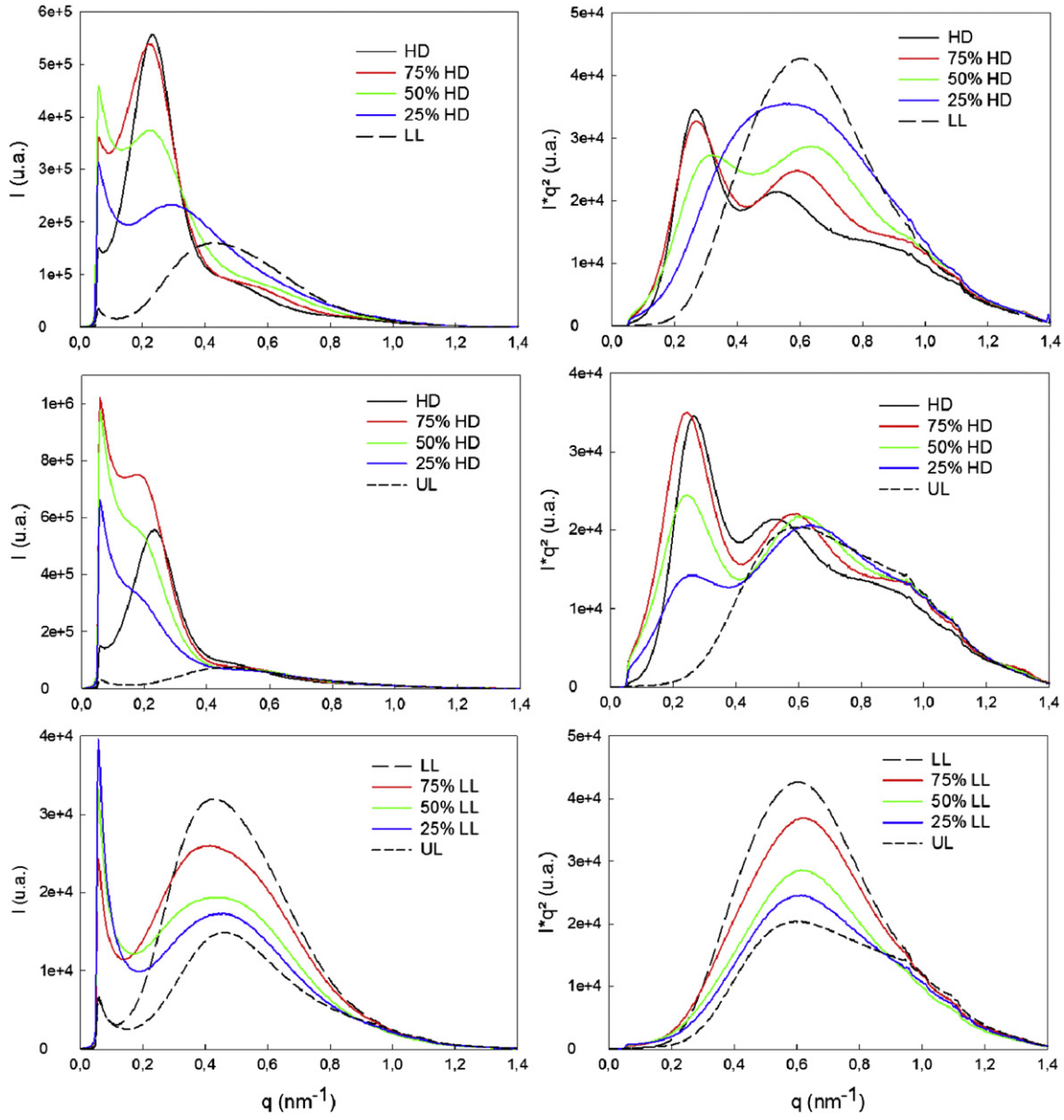

Fig. 11. $I(q)$ and $Iq^2(q)$ SAXS intensity profiles of the three binary systems.

amplitude between the ones of the two contributions. These two long periods give further evidence of the micro-phase separation of the HD and LL components that seem to have crystallized as if alone. The invariant location of the 1st peak with regard to that of the pure HD copolymer is however apparently contradictory with the T_m^{high} drop of this blend. A probable explanation is that the L_c drop due to cocrystallization is compensated by the L_a increase due to the LL chain mixing in the amorphous regions of the HD-rich phase.

Regarding the 50/50 blend, the shift to higher q value of the 1st peak indicates a L_p decrease in the HD-rich phase. This vouchers in favour of a major incidence of the L_c decrease resulting from cocrystallization as compared to the L_a increase, in this blend.

The fact that the 2nd correlation peak for the various blends gradually shifts from the position of the HD 2nd harmonic to the position of the LL single peak confirms the superposition of these two contributions. It does not provide further information on the evolution with composition of the thicknesses of either the crystal lamellae or the amorphous layers in the LL-rich phase due to HD chain solubility and eventually cocrystallization.

The 75/25 blend surprisingly exhibits a single very broad correlation maximum slightly shifted to small q with regard to the pure LL copolymer. This is indicative of a unique L_p value in the lamellar stacking, with a very broad distribution. However, according to the crystallization and melting DSC traces, there are actually two kinds of crystalline lamellae: the thicker ones related to the HD copolymer and the thinner ones akin to the LL copolymer. Several authors reported similar observation for binary systems of high and low crystallinity PE-based polymers. Regarding HDPE-poor blends of HDPE with either LDPE or hydrogenated polybutadiene, Wignall et al. [28,35] assigned the single broad SAXS correlation peak to a common lamellar stack of mixed lamellae, indicating crystallization-induced phase separation from a miscible melt. Tashiro et al. [34] also argued for an aggregate of the unlike lamellae, as assessed from *in situ* SAXS during slow cooling of LLDPE blends with deuterated HDPE. However, studying HDPE–LDPE blends, Reckinger et al. [26] theoretically demonstrated that the characteristic L_p value of a random distribution of the two kinds of lamellae resulting from a crystallization-induced phase separation in a homogeneous melt would be equal to the average of the ones of the two components. In the present study, the observed most probable long period, $L_p \approx 11.4$ nm, in the 75/25 blend is much lower than the computed volume-average value, $L_p \approx 14.0$ nm, of the LL and HD components (10.4 nm and 25.0 nm, respectively). This L_p deviation from Reckinger et al.'s mixing rule strongly suggests that crystallization did not occur in a homogeneous melt, otherwise the solid blend consists of HD-rich domains dispersed in an LL-rich matrix, in agreement with the observation of an intense scattering at small q. In support to this proposal, it is worth noticing the significant broadening of the correlation peak of the blend on its small q side, with regard to that of the pure LL copolymer: this is a hint of the scattering contribution from the HD-rich domains. The missing of a resolved SAXS peak from these HD-rich domains may be simply due to combined effects of weak intensity and high-q shift due to cocrystallization (L_c reduction), as for the two previous blends.

5.3. UL–HD system

The $Iq^2(q)$ intensity profiles of the blends all display two scattering maxima that perfectly corroborate the phase separation of the UL and HD chain species previously concluded from the very high intensity at very low q value of the $I(q)$ curves, at the beginning of this section. There are yet significant differences between the various blends. As for the previous system, the 25/75 blend displays a 1st correlation peak close to that of the HD copolymer and a 2nd one close to that of the UL copolymer. Closer examination of the data reveals that the 1st peak is slightly shifted to small q indicating L_p increase in the HD-rich phase. The same trend is observed for the 50/50 and 75/25 blends, with no further increase of L_p. One may hardly assume a L_c increase of the HD crystallites with increasing UL content in the blends, noticeably considering the T_m^{high} depression. One may yet easily assign the phenomenon to a thickening effect in the amorphous regions of the HD-rich phase (*i.e.*, L_a increase) due to the solubility of UL chains, that compensate the possible L_c drop due to minute cocrystallization.

The fact that the 1st peak from the HD-rich phase is still observable in the 75/25 UL/HD blend, in contrast to the 75/25 LL/HD blend, is not an indication of a different behavior. Two arguments may be brought forth. On the one hand, the scattering intensity contrast is more favorable to the HD component in the UL/HD system. On the other hand, the shift to small q enables this peak to emerge from the base of the broad scattering of the UL copolymer.

Considering the previous observation of a gradual T_m^{high} drop with increasing UL concentration in the blends that suggests L_c reduction due to cocrystallization, the present L_p invariance at a value slightly greater than that of the pure HD copolymer can be assigned to an increasing solubility of UL chains in the amorphous regions of the HD-rich phase that roughly counterbalances the L_c drop. The crystal surface free energy contribution to the T_m^{high} depression may thus be taken as a very probable issue for two reasons: 1) due to their high ξ value, the UL chains dissolved in the amorphous phase of the HD-rich regions should involve a significant increase of σ_e; 2) the cocrystallization capabilities of HD and UL chains should be rather low owing to their large ξ difference.

5.4. UL–LL system

Although the scattering intensity from the UL copolymer is quite lower than that of the LL one, the shape and location of the correlation maximum is very similar for the two components. The $Iq^2(q)$ scattering curves of the blends roughly obey a linear combination of the curves of the pure components. This does not allow arguing about the miscibility and structural behavior of the blends, and about the L_c evolution with composition. Only the strong scattering close to the beam-stop, previously pointed out from the $I(q)$ plots, confirms the phase separation at a scale level far beyond that of the crystalline lamella thickness.

6. AFM structural characterization

It is worth noticing first that there are very few reports dealing with direct structural characterization of PE-based blends at a nanometric scale by transmission electron microscopy [35,88–90] or AFM [91]. The analysis of the micrographs indeed proved to be not so obvious. In the present study, *phase* images turned out more relevant than *height* images for revealing the morphological features from the *native* surface of the films.

AFM images of the copolymers and blends for the LL/HD and UL/LL systems are reported in Fig. 12. The choice of the image scale is a compromise for the best examination of blend morphology in account of the strong difference between the structural scales of the phase-separated domains and that of the components within the domains. For the two binary systems, the blends display a predominance of lamellae akin to the more crystalline copolymer. This is particularly true for the LL/HD systems for which the well-formed HD lamellae seem to invade the sample surface of the blends. Similar unreported observations were made for the UL/HD system. This may be due to the preparation method that promotes

generation on the sample surface of the morphological fingerprint of the component having the higher crystallization capabilities (greater crystal content and higher crystallization kinetics). However, when the lower crystallinity copolymer is predominant, namely the 75–25 blends of each binary systems in Fig. 12, a clear micro-phase separation morphology at a much larger scale than that of the periodic lamellar stacking of the components is observed, in agreement with the preceding conclusions.

7. Dynamic thermomechanical behavior

The storage modulus, E', and loss factor, tan δ, are plotted in Fig. 13 as a function of temperature for the three binary systems UL/LL, UL/HD and LL/HD. The three typical relaxations of PE-based materials can be clearly observed. The γ relaxation that appears in the temperature range (−140/−110 °C) of the tan δ plots is very similar for the three copolymers and their blends, irrespective of their crystallinity index. This is consistent with the assignment to local chain motions in both the crystal and the amorphous regions [92]. The corresponding very small drop of stiffness on the $E'(T)$ plots that contrasts with previous data on linear PE [93] confirms that the γ relaxation is not a cooperative process for the present systems. From a practical standpoint, it is thoroughly useless for miscibility evaluation.

Regarding the β relaxation in the temperature range (−60/−40 °C), the marked $E'(T)$ drop clearly reveals a cooperative process that can be assigned to the main relaxation in the amorphous phase [92]. Mandelkern and collaborators [94,95] concluded that the β relaxation is only a contribution from the interfacial amorphous not the whole amorphous phase. Our assignment yet agrees with studies by Bensason et al. [73,96] of the relaxation behavior of low density metallocene copolymers and their blends. These reports also clearly show that the β relaxation in homogeneous ethylene/α-olefin copolymers gradually shifts to higher temperature with increasing crystallinity, up to merging into the α relaxation [73,96].

The LL/HD and UL/HD blends exhibit a monotonic increase of the β-peak amplitude with LL and UL content, respectively, without significant temperature shift. This insensitivity of LL or UL chain mobility to blending with HD, even when the latter component is predominant, is a hint of phase separation in the amorphous regions of the blends that support micro-phase separation prior to crystallization. Similar situation and conclusion have been made by Bensason et al. [73] regarding blends of various homogeneous copolymers.

The UL/LL system is more complex since it exhibits a β-peak shift only for the 25/75 blend, indicating at least partial miscibility in the amorphous regions of this blend. This suggests a higher degree of miscibility in the melt for LL-rich blend, in rough agreement with the present rheological data (positive η_0 deviation), as well as with Hill–Braham's observation that melt miscibility prevails in the low ξ copolymer side of the phase diagram.

The α relaxation assigned to the motional activation of conformational chain defects in the crystal [97], probably combined with mobility of chain folds, appears in a wide temperature range beyond 20 °C [92]. If the amplitude of the α relaxation mainly depends on crystallinity, the prime dependence factor of the α-peak temperature is the crystal thickness [95,98].

All three systems display a collapse of the elastic modulus in the high temperature range resulting from both the gradual mechanical softening of the crystals with increasing temperature and their final melting. However, only the UL/LL system exhibits a clear evolution with composition of the α relaxation on the tan δ plots. The α-peak temperature depression of the 75/25 blend is quite consistent with the crystal thickness reduction resulting from cocrystallization. By contrast, the slightly positive shift of the α-peak temperature of the 25–75 blend beyond that of the pure LL copolymer suggests that the crystals are thicker in the blend. Duplication of the DMTA experiments in tensile mode, and experiments in torsion mode as well, confirmed this unusual phenomenon. This is yet quite consistent with the observation that T_m^{high} of the 25–75 UL/LL blend is slightly higher than that of the pure LL copolymer. The previous explanation regarding this T_m^{high} evolution relies on the interfacial nucleation effect that promoted an early crystallization in the LL-rich phase.

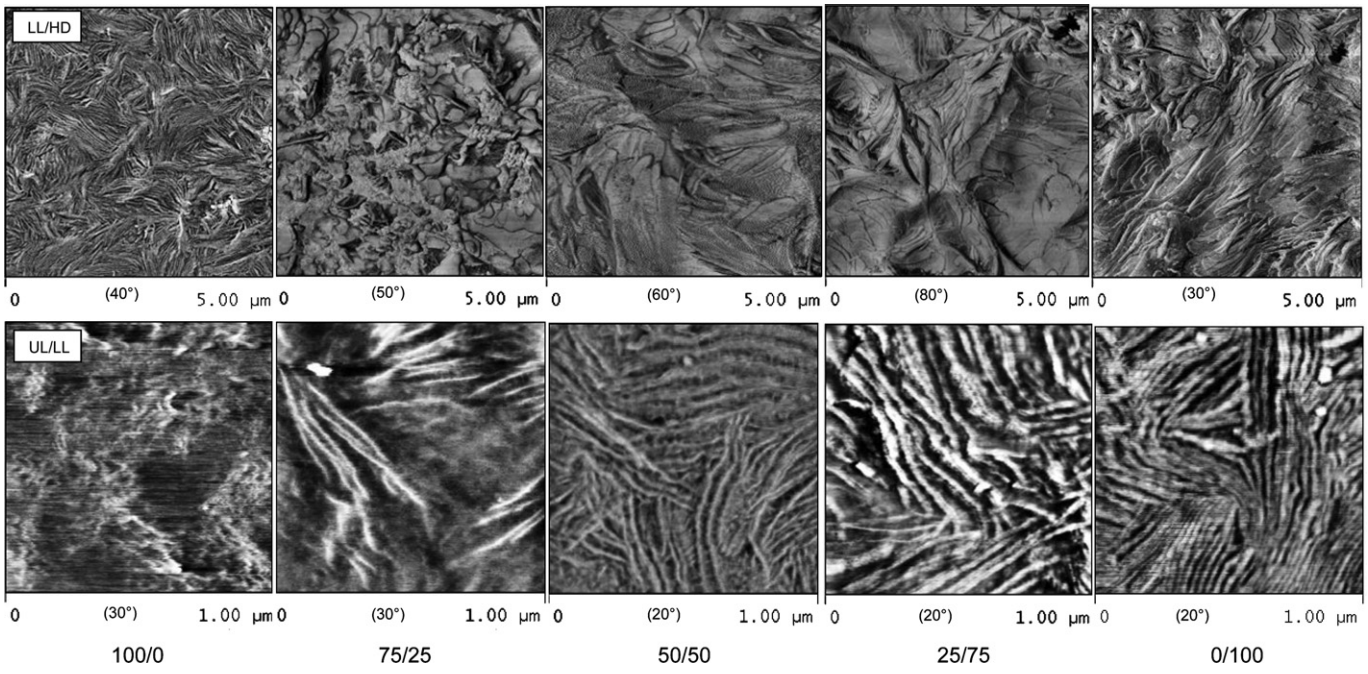

Fig. 12. AFM *phase* images of the copolymers and blends of the LL/HD and UL/LL binary systems (between brackets is indicated the phase amplitude for every image).

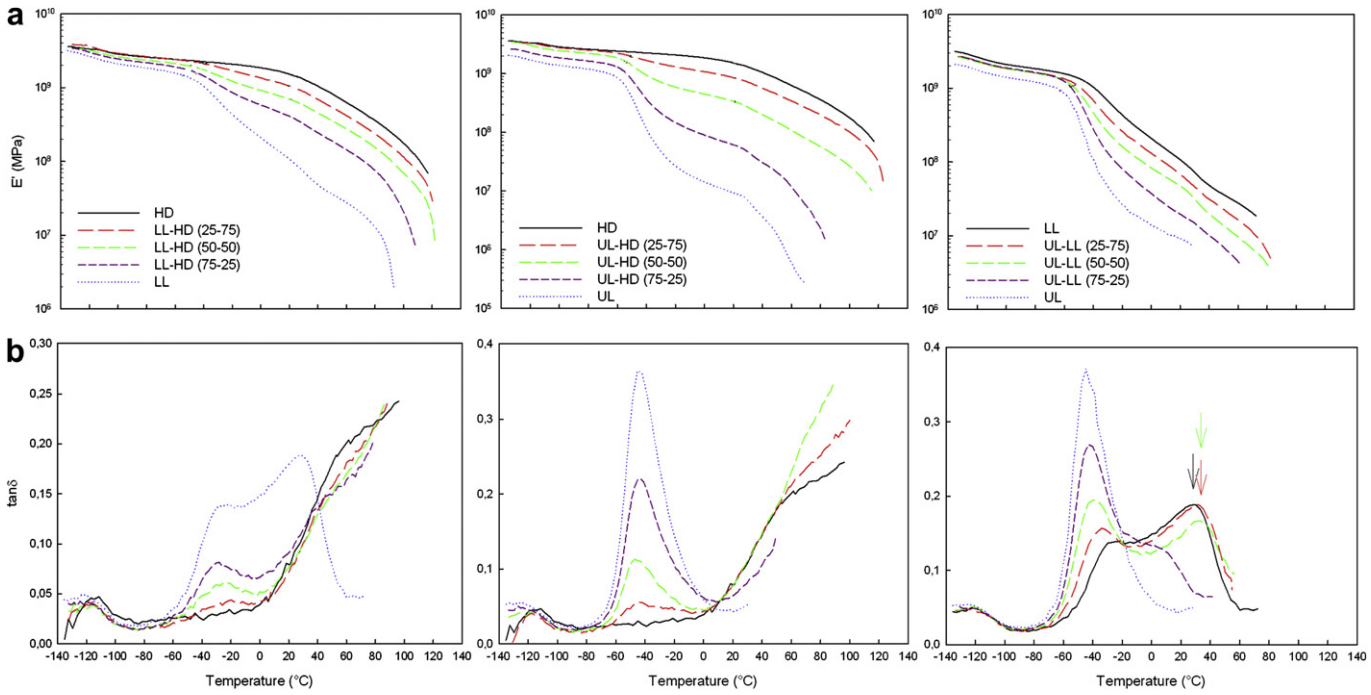

Fig. 13. DMTA of the three binary systems: (a) storage modulus, E', and (b) loss factor, tan δ, as a function of temperature.

8. Concluding discussion

The emulsion-like rheological behavior of the three systems of the present study suggests immiscibility over the whole composition domain. However, the dual behavior of negative and positive η_0 deviation is indicative of either total lack of interactions at the interface of the phase-separated domains or strong interactions through miscibility and/or composition gradient. These conclusions are consistent, though not in perfect agreement, with Hill—Barham's studies reporting that miscibility and a phase separation loop systematically occurs in the counit-rich copolymer side of the phase diagram for a great variety of binary PE-based systems. The strong interactions evidenced through the positive η_0 deviation on the high ξ copolymer side of the phase diagram decrease with increasing ξ difference of the components of the binary blends. This contrasts with Hill—Braham's conclusions that the size of the miscibility domain increases upon increasing ξ difference of the components.

The whole set of DSC data provides evidence that phase separation of the unlike species also prevails in the solid state, with partial miscibility between the phase-separated domains that depends on the ξ difference of the components in each binary system. Partial miscibility either in the amorphous phase or in the crystalline phase via cocrystallization decreases with increasing ξ difference of the copolymers in the order: UL/LL > LL/HD > UL/HD. This suggests that the driving force to the phenomenon is the amount of homologous chains having close ξ values in the unlike copolymers, owing to the chemical heterogeneity that is even present in the metallocene materials. The three systems display a systematic positive T_c^{high} deviation to the linear relationship, due to an interfacial nucleation-promoted crystallization of the phase rich in low ξ copolymer, *i.e.,* the HT melting phase. The concomitant depression of the T_m^{high} with decreasing content of low ξ copolymer in the blends is assigned to combined cocrystallization-induced reduction of crystal thickness and surface free energy increase due to solubility of the high ξ species in both the crystalline and amorphous regions of the HT melting phase. The T_m^{high} value slightly higher than that of the components in the UL/LL system suggests that early nucleation results in thicker crystals in the HT melting phase. *Hybrid* crystals with melting point intermediate between those of the two major phases have been assigned to a gradient composition, the amount of which increases upon decreasing ξ difference of the components. The DSC data yet do not *per se* provide direct evidence that phase separation took place prior to crystallization for the present blend preparation conditions, they just suggest it. Besides, the DSC data do not provide any information that could help understanding the dual rheological behavior.

Evidence from SAXS of electron density fluctuations at a much larger scale than that of the crystal thickness in the blends of the three binary systems provides demonstration that phase separation had already occurred in the melt prior to crystallization. The double long period distribution corroborates this conclusion for the LL/HD and UL/HD systems. Long period variations in the HD-rich phase of both systems corroborate the solubility of high ξ copolymer chains in the HD-rich phase that thickens the amorphous layer (for both LL/HD and UL/HD) and reduces the crystal thickness via cocrystallization (for LL/HD).

DMTA and AFM roughly confirm micro-phase separation. Besides, DMTA gives support to the crystal thickness increase in the 25/75 UL/LL blend with regard to the pure LL copolymer as suggested from the melting behavior.

Acknowledgments

The authors are indebted to Total Petrochemicals (Feluy, Belgium) and Dow Chemicals (Terneuzen, The Netherlands) for the supply of the high density polyethylene and the metallocene copolymers, respectively, together with their molecular characteristics. The European Synchrotron Radiation Facility (Grenoble, France) is deeply acknowledged for access and accommodation on the BM2-D2AM beamline.

References

[1] Soares JBP. Chem Eng Sci 2001;56:4131–53.
[2] Peacock AJ. Handbook of polyethylene: structures, properties, and applications. New York: Marcel Dekker Inc.; 2000.
[3] Knuuttila H, Lehtinen A, Salminen H. In: Schiers J, Kaminsky W, editors. Metallocene-based polymers: preparation, properties and technology, vol. 2. New York: Wiley-Interscience; 1999.
[4] Popli R, Mandelkern L. J Polym Sci Polym Phys 1987;25:441–83.
[5] Crist B, Fisher CJ, Howard PR. Macromolecules 1989;22:1709–18.
[6] Séguéla R, Rietsch F. Polymer 1986;27:703–8.
[7] Hosoda S, Uemura A. Polym J 1992;24:939–49.
[8] Rose LJ, Channel AD, Frye CJ, Capaccio G. J Appl Polym Sci 1994;54:2119–24.
[9] Kennedy MA, Peacock AJ, Mandelkern L. Macromolecules 1994;27:5297–310.
[10] Kennedy MA, Peacock AJ, Failla MD, Lucas JC, Mandelkern L. Macromolecules 1995;28:1407–21.
[11] Berthold J, Böhm LL, Enderle H-F, Gobel P, Luker H, Lecht R, et al. Plast Rubber Process Appl 1996;25:368–72.
[12] Soares JBP, Abbott RF, Kim JD. J Polym Sci Polym Phys 2000;38:1267–75.
[13] Guichon O, Séguéla R, David L, Vigier G. J Polym Sci Polym Phys 2003;41:327–40.
[14] Séguéla R. Macromol Mater Eng 2007;292:235–44.
[15] Utracki LA. J Rheol 1991;35:1615–37.
[16] Utracki LA. Symp Ser 1989;395:153–210.
[17] Zhao L, Choi P. Mater Manuf Process 2006;21:135–42.
[18] Schipp C, Hill MJ, Barham PJ, Cloke VW, Higgins JS, Oiarzabal L. Polymer 1996;37:2291–7.
[19] Wignall GD, Alamo RG, Londono JD, Mandelkern L, Stehling FC. Macromolecules 1996;29:5332–5.
[20] Alamo RG, Graessley WW, Krishnamoorti R, Lohse DJ, Londondo JD, Mandelkern L, et al. Macromolecules 1997;30:561–6.
[21] Reichart GC, Graessley WW, Register RA, Lohse DJ. Macromolecules 1998;31:7886–94.
[22] Wignall GD, Alamo RG, Ritchson EJ, Mandelkern L, Schwahn D. Macromolecules 2001;34:8160–5.
[23] Hill MJ, Barham PJ. Polymer 1995;36:3369–75.
[24] Morgan RL, Hill MJ, Barham PJ. Polymer 1999;40:337–48.
[25] Wang S, Wu C, Ren M-Q, van Horn RM, Graham MJ, Han CC, et al. Polymer 2009;50:1025–33.
[26] Reckinger C, Larbi FC, Rault J. J Macromol Sci Phys 1984;B23:511–26.
[27] Alamo RG, Glazer RH, Manderkern L. J Polym Sci Polym Phys 1988;26:2169–95.
[28] Wignall GD, Londondo JD, Lin JS, Alamo RG, Galante MJ, Mandelkern L. Macromolecules 1995;28:3156–67.
[29] Galante MJ, Mandelkern L, Alamo RG. Polymer 1998;39:5105–19.
[30] Anantawaraskul S, Soares JBP, Wood-Adams PM. Macromol Chem Phys 2004;205:771–7.
[31] Xu J, Xu X, Chen L, Feng L, Chen W. Polymer 2001;42:3867–74.
[32] Hussein IA, Hammed T, Sharkh BFA, Mezghani K. Polymer 2003;44:4665–72.
[33] Gaucher V, Séguéla R. Polymer 1994;35:2049–55.
[34] Tashiro K, Satowski MM, Stein RS, Li Y, Chu B, Hsu SL. Macromolecules 1992;25:1809–15.
[35] Wignall GD, Alamo RG, Londono JD, Mandelkern L, Kim MH, Lin JS, et al. Macromolecules 2000;33:551–61.
[36] Rana D, Kim HL, Kwag H, Choe S. Polymer 2000;41:7067–82.
[37] Usami T, Gotoh Y, Takayama S. Macromolecules 1986;19:2722–6.
[38] Schouterden P, Groeninckx G, van der Heijden B, Jansen F. Polymer 1987;28:2099–104.
[39] Mathot VBF, Pijpers MFJ. J Appl Polym Sci 1990;39:979–94.
[40] Wilfong DL, Knight GW. J Polym Sci Polym Phys 1990;28:861–70.
[41] Hosoda S. Polym J 1988;20:383–97.
[42] Anantawaraskul S, Soares JBP, Wood-Adams PM. Adv Polym Sci 2005;182:1–54.
[43] Hubert L, David L, Séguéla R, Vigier G, Degoulet C, Germain Y. Polymer 2001;42:8425–34.
[44] Cazenave J, Séguéla R, Sixou B, Germain Y. Polymer 2006;47:3904–14.
[45] Krishnaswamy RK, Yang Q, Fernandez-Ballester L, Kornfield JA. Macromolecules 2008;41:1693–704.
[46] Puig CC, Odell JA, Hill MJ, Barham PJ, Folkes MJ. Polymer 1994;35:2452–7.
[47] Bensason S, Nazarenko S, Chum S, Hiltner A, Baer E. Polymer 1997;38:3913–9.
[48] Neway B, Gedde UW. J App Polym Sci 2004;94:1730–6.
[49] Carreau PJ, De Kee D, Chhabra RP. Rheology of polymeric systems: principles and applications. Munich: Hanser; 1997.
[50] Wunderlich B. Macromolecular physics. In: Crystal melting, vol. 3. New York: Academic Press; 1980.
[51] Verstrate G, Wilchinsky ZW. J Polym Sci Polym Phys 1974;9:127–42.
[52] Martinez-Salazar J, Sanchez-Cuesta M, Balta-Calleja F-J. Colloid Polym Sci 1987;265:239–45.
[53] Schultz JM. Polymer materials science. Englewood Cliffs: Prentice-Hall; 1974.
[54] Ferreiro V, Coulon G. J Polym Sci Polym Phys 2004;42:687–701.
[55] Hill MJ, Barham PJ. Polymer 2000;41:1621–5.
[56] Fang Y, Carreau PJ, Lafleur PG. Polym Eng Sci 2005;45:1254–64.
[57] Delgadillo-Velasquez O, Hatzikiriakos SG, Sentmanat M. J Polym Sci Polym Phys 2008;46:1669–83.
[58] Rana D, Kim HL, Kwag H, Rhee J, Cho K, Woo T, et al. J Appl Polym Sci 2000;76:1950–64.
[59] Kim MS, Kim BK. Polym Adv Technol 2004;15:419–24.
[60] Al-Malaika S, Kong W. Polymer 2005;46:209–28.
[61] Wei Q, Donatella CD, Pracella M. Macromol Chem Phys 2005;206:777–86.
[62] Bulamurugan G, Maiti SN. Polym Eng Sci 2008;48:2482–98.
[63] Liu Y-L, Yin L-G, Ke Z, Shi Q, Yin J-H. e-Polymers 2009;074:11.
[64] Hill MJ, Barham PJ, Keller A, Rosney CCA. Polymer 1991;32:1384–93.
[65] Hill MJ, Barham PJ. Polymer 1992;33:4099–107.
[66] Hill MJ, Barham PJ, van Ruiten J. Polymer 1993;34:2975–80.
[67] Kwak H, Rana D, Choe S. J Ind Eng Chem 2000;6:107–14.
[68] Guimaraes JMO, Coutinho FMB, Rocha MCG, Farah M, Bretas RES. J Appl Polym Sci 2002;86:2240–6.
[69] Lee PC, Park HE, Morse DC, Macoscko CW. J Rheol 2009;53:893–915.
[70] Zhao R, Macoscko CW. J Rheol 2002;46:145–67.
[71] Soares JBP, Kim JD, Rempel GL. Ing Eng Chem Res 1997;36:1144–50.
[72] Xu J, Xu X, Feng L, Chen L, Chen W. Macromol Chem Phys 2001;202:1524–30.
[73] Bensason S, Minick J, Moet A, Chum S, Hiltner A, Baer E. J Polym Sci Polym Phys 1996;34:1301–15.
[74] Xu X, Xu J, Chen L, Liu R, Feng L. J Appl Polym Sci 2001;80:123–9.
[75] Mathot VBF, Scherrenberg RL, Pijpers TFJ. Polymer 1998;39:4541–59.
[76] Séguéla R. J Polym Sci Polym Phys 2005;43:1729–48.
[77] Darras O, Séguéla R. Polymer 1993;34:2946–50.
[78] Muratoglu OK, Argon AS, Cohen RE, Weinberg M. Polymer 1995;36:921–30.
[79] Arroyo M, Zitzumbo R, Avalos F. Polymer 2000;41:6351–9.
[80] Calvao PS, Chenal J-M, Gauthier C, Demarquette NR, Dos Santos AM, Cavaille J-Y. Polym Inter 2010;59. doi:10.1002/pi.2799.
[81] Barham PJ, Jarvis DA, Keller A. J Polym Sci Polym Phys 1982;20:1733–48.
[82] Schaaf P, Lotz B, Wittmann JC. Polymer 1987;28:193–200.
[83] Muratoglu OK, Argon AS, Cohen RE. Polymer 1995;36:2143–52.
[84] Laurens C, Ober R, Creton C, Leger L. Macromolecules 2004;37:6806–13.
[85] Loos J, Katzenberg F, Petermann J. J Mater Sci 1997;32:1551–4.
[86] Puig CC. Polym Bull 1997;38:715–20.
[87] Isasi JR, Haigh JA, Graham JT, Mandelkern L, Alamo RG. Polymer 2000;41:8813–23.
[88] Norton DR, Keller A. J Mater Sci 1984;19:447–56.
[89] Conde Braña MT, Iragorri Sainz JI, Terselius B, Gedde UW. Polymer 1989;30:410–5.
[90] Conde Braña MT, Gedde UW. Polymer 1992;33:3123–36.
[91] Adhikari R, Godehardt R, Lebek W, Michler GH. J Appl Polym Sci 2007;103:1887–93.
[92] Hoffman JD, Williams G, Passaglia E. J Polym Sci Polym Symp 1966;14:173–235.
[93] Stheling F, Mandelkern L. Macromolecules 1970;3:242–52.
[94] Popli R, Mandelkern L. Polym Bull 1983;9:260–7.
[95] Popli R, Glotin M, Mandelkern L. J Polym Sci Polym Phys 1984;22:407–48.
[96] Bensason S, Nazarenko S, Chum S, Hiltner A, Baer E. Polymer 1997;38:3513–20.
[97] Boyd RH. Polymer 1985;26:1123–33.
[98] Takayanagi M, Matsuo T. J Macromol Sci Phys 1967;B1:407–31.